*Nanotoxicology*, 2012; Early Online, 1–13

ISSN: 1743-5390 print / 1743-5404 online
DOI: 10.3109/17435390.2011.653416

informa
healthcare

# *In vitro* assessment of engineered nanomaterials using a hepatocyte cell line: cytotoxicity, pro-inflammatory cytokines and functional markers

Ali Kermanizadeh[1], Giulio Pojana[2], Birgit K Gaiser[1], Renie Birkedal[3], Dagmar Bilaničová[2], Håkan Wallin[3], Keld Alstrup Jensen[3], Börje Sellergren[4], Gary R Hutchison[5], Antonio Marcomini[2] & Vicki Stone[1]

[1]*Heriot-Watt University, School of Life Sciences, John Muir Building, Edinburgh, UK,* [2]*Department of Environmental Sciences, Informatics and Statistics, University Ca' Foscari Venice, Venice, Italy,* [3]*National Research Centre for the Working Environment, Copenhagen, UK,* [4]*Institute für Umweltforschung (INFU), Technical University of Dortmund, Dortmund, Germany and* [5]*Edinburgh Napier University, School of Life, Sport and Social Sciences, Sighthill Campus, Sighthill Court, Edinburgh, UK*



**Abstract**

**Effects on the liver C3A cell line treated with a panel of engineered nanomaterials (NMs) consisting of two zinc oxide particles (ZnO; coated 100 nm and uncoated 130 nm), two multi-walled carbon nanotubes (MWCNTs), one silver (Ag < 20 nm), one 7 nm anatase, two rutile $TiO_2$ nanoparticles (10 and 94 nm) and two derivatives with positive and negative covalent functionalisation of the 10 nm rutile were evaluated. The silver particles elicited the greatest level of cytotoxicity (24 h LC50 – 2 μg/cm$^2$). The silver was followed by the uncoated ZnO (24 h LC50 – 7.5 μg/cm$^2$) and coated ZnO (24 h LC50 – 15 μg/cm$^2$) particles with respect to cytotoxicity. The ZnO NMs were found to be about 50–60% soluble which could account for their toxicity. By contrast, the Ag was <1% soluble. The LC50 was not attained in the presence of any of the other engineered NMs (up to 80 μg/cm$^2$). All NMs significantly increased IL-8 production. Meanwhile, no significant change in TNF-α, IL-6 or CRP was detected. Urea and albumin production were measured as indicators of hepatic function. These markers were only altered by the coated and uncoated ZnO, which significantly decreased albumin production.**

**Keywords:** Liver, inflammation, IL-8, albumin, urea

## Introduction

The rapid expansion of technological, scientific and commercial uses of atomic or molecular scale materials, their assembly and their unique properties, has led to an escalating interest in the fields of nanoscience and nanotechnology (Maynard et al. 2006). In 2011, there were over 1300 consumer products on the market that claimed to contain elements of nanotechnology (Woodrow Wilson website).

However, due to their unique chemical and physical properties, there is concern that some nanomaterials (NMs) could be hazardous for people living and working with these particles (Hoet et al. 2004). The small size of particulate NMs results in high surface area to volume ratio, which potentially offers a greater biological activity per given mass compared with larger-size particles (Oberdorster et al. 2005). In addition to this, the surface reactivity per unit surface area may be even greater at the nanoscale.

Conventional risk assessment paradigms require evaluation of the potential hazard and exposure (dose). However, in studies of engineered pigments and NMs it has been realised that the results may not be extrapolated due to insufficient or inaccurate physicochemical characterisation of the test materials. Consequently, in particle toxicology detailed information about the specific materials and their behaviour in the test systems may be equally important (Hoet et al. 2004; Sandhiya et al. 2009). Any comprehensive testing of particle toxicity should include information on parameters such as surface area, surface chemistry, size distribution and surface charge (Oberdorster et al. 2005). It is likely that each NM will differ in the levels of toxicity induced and the mechanism by which they exert these adverse effects. Hence, in this study a panel of 10 engineered NMs including suspended Ag, coated and uncoated ZnO, five different $TiO_2$ NPs (all different sizes or crystal form and/or surface coating) and two multi-walled carbon nanotubes (MWCNTs) were utilised. The use of such a diverse panel of NMs allowed for comparison of a wide variety of physicochemical characteristics with different biological activity and toxicity.

Nanosilver is widely utilised as an additive in various textiles and plastics due to its antimicrobial properties. It is also used for treatment of wounds and burns or as a contraceptive, as well as being marketed as a water disinfectant (Chen et al. 2008). Since Ag NPs are regularly utilised in water disinfection and food preservation there is a real possibility that such particles may be ingested by humans and therefore

Correspondence: Ali Kermanizadeh, Heriot Watt University, School of Life Sciences, John Muir Building, Edinburgh, EH14 4AS, UK. Tel: +0131 4514313. E-mail: Ak435@hw.ac.uk

*(Received 13 June 2011; accepted 22 December 2011)*

reach the gastrointestinal tract. Once ingested there is potential for material uptake, for example, by Peyer's patches or enterocytes (Buzea et al. 2007; Gaiser et al. 2009). It has been suggested that, once in the sub-mucosal tissue, silver NPs are able to enter the lymphatics and capillaries (Takenaka et al. 2001). There is some evidence that ingested NMs can have an impact on the liver (Takenaka et al. 2001). Following inhalation and tracheal instillation silver particles of 15 nm were found to rapidly decrease in number in the lung due to clearance (Takenaka et al. 2001). These particles were later observed in the blood and other organs including the liver and the kidneys (Takenaka et al. 2001). Similarly, elevated levels of silver was found in the liver as well as the kidney, lung and the brain after repeated gastrointestinal exposure to both 14 nm silver NPs and silver acetate. In this case, exposure to dissolved silver NPs resulted in considerably lower concentration of the Ag in the organs, however, the distribution pattern was unaffected (Loeschner et al. 2011). These studies indicate that the liver is a relevant target for ingested and inhaled silver NPs.

ZnO NPs have been shown to have great benefits in society and are currently being applied in a broad range of industries including cosmetics (sunscreens), biosensors and numerous electronic goods (Deng et al. 2009). Furthermore, due to their antibacterial properties, these particles have huge potential in the development of prophylactic drugs (Huang et al. 2008). Many studies have focused on the influence of ZnO NPs on bacterial growth. An example of one such study demonstrates that ZnO severely inhibits the growth of *Escherichia coli* and protects intestinal cells from an enterotoxigenic form of the bacteria (Roselli et al. 2003), while another group have publicised that the particulate has bacteriostatic effects against *Staphylococcus aureus* and *Streptococcus agalactiae* (Huang et al. 2008).

$TiO_2$ NMs have a wide range of uses including functional fillers in paint, paper, plastics, food additives and colorants, as well as in pharmaceutical and cosmetic industries (Jin et al. 2008). In addition, due to the unique ability of anatase $TiO_2$ NPs to absorb UV light with very low scattering, it is widely utilised in sunscreen products and self-cleaning windows (Jin et al. 2008). Previous studies have shown that the uptake and translocation of $TiO_2$ following intratracheal instillation have resulted in accumulation of NMs within the liver (Semmler-Behnke et al. 2008; Geiser et al. 2010). The same group has also found hepatic accumulation of $TiO_2$ following gavage exposure of rats (Semmler-Behnke et al. 2008). These studies therefore also demonstrate the relevance of the liver as the target of $TiO_2$ exposure.

Carbon nanotubes consist of single-walled (SWCNT) or several layers (MWCNT) of graphene sheets, rolled up into seamless tubes with a diameter in the nanometer scale. These materials have unique physical and chemical properties making them an ideal candidate in a multitude of industrial applications including high resistance composites and electronic devices (De Nicola et al. 2009). Carbon nanotubes are also being developed for use as diagnostic and therapeutic tools for the detection and treatment of diseases including certain cancers requiring their systemic administration (Ferrari et al. 2005).

Based on previous literature, it is widely demonstrated that NMs administered via intravenous routes will eventually reach the liver (Chen et al. 1999; Sadauskas et al. 2009). This organ is of utmost importance, as it has been shown to accumulate NMs at high concentrations compared with other organs (Sadauskas et al. 2009) and alongside the kidneys might be responsible for the clearance of NMs from the blood (Chen et al. 1999; Sadauskas et al. 2009). The liver is characterised by its distinct populations of cells, each with their own unique morphology and function. Of particular interest are the hepatocytes, due to their abundance and their importance in the normal liver function. Hepatocytes are also known to synthesise many hormones and cytokines including interleukin 8 (IL-8) (Dong et al. 1998), interleukin 6 (IL-6) (Saad et al. 1995) and tumour necrosis factor-α (TNF-α) (Dong et al. 1998; Saad et al. 1995).

This *in vitro* study investigated the potential of the investigated engineered NMs to induce cytotoxicity, measured by mitochondrial function using WST-1 and AlamarBlue assays, and to induce an inflammatory response in the hepatoblastoma cell line C3A, measured by the release of pro-inflammatory cytokines (IL-6, IL-8 and TNF-α). C-reactive protein (CRP) levels were also measured following hepatocyte exposure to the NMs. CRP is a member of the class of acute-phase reactants produced by the hepatocytes in response to foreign substances and its levels rise dramatically during inflammatory processes (Rhodes et al. 2011).

As indicators of hepatocyte function, we investigated the effects of NM exposure on albumin and urea production. Albumin is the most abundant hepatic-derived serum protein. Serum albumin levels have been linked to several diseases. Low albumin levels can suggest liver and kidney disease, inflammation, shock and malnutrition (Gekle 2005).

The work in this study is part of a larger European study: ENPRA (Risk Assessment of Engineered Nanoparticles). Many of the materials were provided by the OECD (Organisation for Economic Co-operation and Development) programme of NMs health and safety research, allowing comparison with a wider body of research and characterisation in the future (all materials with the prefix code "NM" are included in the OECD programme). The samples donated NRCWE (National Research Centre for the Working Environment) were produced to address specific questions about the toxicological role of crystal phase, size and surface charge. The results of this *in vitro* study will ultimately feed into a risk assessment for these materials.

## Methods

### Nanomaterials

NMs were purchased as stated: NM 101 (Hombikat UV100; rutile with minor anatase; 7 nm), NM 110 (BASF Z-Cote; zinkite, uncoated, 100 nm), NM 111 (BASF Z-Cote; zinkite coated with triethoxycaprylylsilane, 130 nm), NM 300 (RAS GmbH; Ag capped with polyoxylaurat Tween-20 <20 nm), NM 400 (Nanocyl; entangled MWCNT, diameter 30 nm), NM 402 (Arkema Graphistrength C100; entangled MWCNT, diameter 30 nm). The above-mentioned NMs were subsampled under Good Laboratory Practice conditions and

preserved under argon in the dark until use. These NMs were received from the European Commission Joint Research Centre (Ispra, Italy). The NRCWE samples were procured by the National Research Centre for the Working Environment. Sub-sampling was completed into 20 ml Scint-Burk glass pp-lock with Alu-Foil (WHEA986581; Wheaton Industries Inc., Millville, NJ, USA) after pooling and mixing 0.1–1 kg of the material to cover the need of the ENPRA project. NRCWE 001, $TiO_2$ rutile 10 nm was purchased from NanoAmor (Houston, TX, USA) and also used for production of NRCWE 002 ($TiO_2$ rutile 10 nm with positive charge) and NRCWE 003 ($TiO_2$ rutile 10 nm with negative charge) using the procedures described below. NRCWE 004 ($TiO_2$ rutile 94 nm) was purchased from NaBond Technologies Co., China. The complete list of investigated NMs including information provided by the suppliers is reported in Table I.

## Surface functionalisation of $TiO_2$

Three hundred g of 10 nm-sized rutile $TiO_2$ (NRCWE 001) was suspended in 1.5 l of 20% methanol in water. The suspension was stirred and 250 ml of 3-aminopropyltriethoxysilane (purity 99%, Sigma-Aldrich, Glostrup, Denmark) was added slowly. The reaction was sonicated with a Branson Sonifier S-450D (Branson, Danbury, CT, USA) mounted with a disruptor horn, on ice at full power for 1 h with 10 s on and 10 s off cycles. The suspension was stirred for 24 h at room temperature. The $TiO_2$ product was collected and was washed sequentially with 100%, 50%, 20%, 10% and 0% methanol in water by centrifugation for 30 min at 35,000 *g*. The material was dried for 2 days at 110°C. The recovery product was 267 g of amino-$TiO_2$.

One hundred and thirty-six g of amino-$TiO_2$ (NRCWE 002) was suspended in 200 ml dry toluene in a three-necked round bottom flask. One hundred g of succinic anhydride (99%, Sigma-Aldrich, Glostrup, Denmark) in 200 ml of dry tetrahydrofuran was added slowly and the reaction was sonicated (see above). The reaction was refluxed for 36 h and the product was collected on a fine porosity glass filter funnel under a slight negative pressure. The product was washed by centrifugation (see above) twice in 100% and once in each 50% methanol, 0.1 M sodium acetate and twice in water. It was dried at 80°C for 2 days. The recovery amount was 90 g.

The zeta potential of the amino-$TiO_2$ was +35 mV and of the carboxy-$TiO_2$ was −29 mV at pH 7.4 in water (Malvern Nano ZetaSizer, Malvern Instruments, Malvern, UK) and it was stable over 24 h.

## Nanomaterial characterisation

Phase compositions and average crystallite sizes were determined by powder X-ray diffractograms obtained at room temperature (25°C) using a Bruker D8 Advanced diffractometer in reflection mode with Bragg-Brentano geometry. A sealed Cu X-ray tube was run at 40 kV and 40 mA, wavelength Cu Kα1 1.5406 Å from a primary beam Ge monochromator, fixed divergence slit 0.2°, step size 0.02, step time 1 s $step^{-1}$, linear position sensitive detector (PSD) (Lynx-eye) with opening angle 3.3°. The sample holders used for the reflection data were either a standard sample holder containing an approximately 2 mm thick sample or a single Si sample holder. One NM 300 sample was measured as transmission in a capillary. The phases were identified by using the EVA 14.0 software from Bruker AXS (copyright 1996–2007 Bruker AXS, Madison, USA). The ratios and sizes were calculated using Topas 4.1 from Bruker (copyright 1999, 2008 Bruker AXS).

Primary and aggregate size range, shape and crystal structure of the test materials were determined by transmission electron microscopy (TEM, JEM-3010, Jeol, Tokyo, Japan) operating at 300 kV. Surface areas and pore volumes were obtained by nitrogen adsorption on a Micrometritics ASAP2000 Accelerated Surface Area and Porosimetry System at an adsorption temperature of -196°C, after pre-treating the sample under high vacuum at 300°C for 2 h (Brunauer et al. 1938). The selected degassing conditions may affect the coating on some of the powder NMs.

The hydrodynamic size distributions of the NMs dispersed in biological media were determined in the 0.128–0.256 mg/ml concentration range (lower concentrations were too low for DLS measurements) by dynamic light scattering (DLS) using a Nicomp Submicron Particle Sizer Autodilute® Model 370 (Santa Barbara, CA, USA). The employed instrument can automatically recognise, in the

Table I. List of engineered NMs investigated, with the original source codes, the nominal sizes and properties as provided by the supplier.

| NM | NM code | Average size (nm) (supplier information) | Additional information | CAS number |
|---|---|---|---|---|
| $TiO_2$ | NM 101 | 7 nm | Anatase, thermal | 13463-67-7 |
| ZnO | NM 110 | 100 nm | uncoated | 1314-13-2, *EINECS* 215-222-5 |
| ZnO | NM 111 | 130 nm | Triethoxycaprylylsilane coated | 1314-13-2, 2943-75-1 *EINECS* 215-222-5, 220-941-2 |
| Ag | NM 300 | <20 nm | Polyoxylaurat Tween-20 capped | 7440-22-4 |
| MWCNT | NM 400 | 30 nm 5 μm long | Short entangled | 7782-42-5, *EINECS* 231-955-3 |
| MWCNT | NM 402 | 30 nm 5 μm long | Long entangled | 7782-42-5, *EINECS* 231-955-3 |
| $TiO_2$ | NRCWE 001 | 10 nm (XRD) | Rutile | 13463-67-7 |
| $TiO_2$ | NRCWE 002 | 10 nm (XRD) | Rutile | – |
| $TiO_2$ | NRCWE 003 | 10 nm (XRD) | Rutile | – |
| $TiO_2$ | NRCWE 004 | 94 nm (XRD) | Rutile | 13463-67-7 |

CAS, Chemical Abstracts Service Registry Numbers; EINECS, European Inventory of Existing Commercial Chemical Substances; MWCNT, multi-walled carbon nanotube; NM, nanomaterial; NRCWE, National Research Centre for the Working Environment; XRD, X-ray diffractogram.

0.5–6000 nm range, up to three size distributions of materials concurrently present through a patented software algorithm. No significant size differences were found at different concentration levels.

### Cell culture and NM treatment

The human hepatoblastoma C3A cell line was obtained from the American Type Culture Collection (ATCC) (Manassas, VA, USA). The cells were maintained in Minimum Essential Medium Eagle (MEM, Invitrogen, Paisley, UK) with 10% foetal calf serum (FCS), 2 mM L-glutamine, 100 U/ml penicillin/streptomycin, 1 mM sodium pyruvate and 1% non-essential amino acids (termed complete medium), at 37°C and 5% $CO_2$.

The Ag was supplied in de-ionised water (85%) with 7% stabilising agent (ammonium nitrate) and 8% emulsifiers (4% each of polyoxyethylene glycerol trioleate and Tween-20). All other materials were supplied as dry powders. NMs were dispersed in Milli-Q de-ionised water with 2% FCS. For coated ZnO, the particles were wetted with 0.5% vol ethanol before the addition of the dispersion media. The NMs were sonicated for 16 min without pause following the protocol developed for ENPRA (Jacobsen et al. 2010; Jensen et al. in preparation). Following the sonication step, all samples were immediately transferred to ice water.

To ascertain the toxicity of NMs to C3A cells 10 concentrations between 0.16 and 80 μg/cm$^2$ were utilised (corresponding to 0.5–256 μg/ml) by diluting in medium containing 10% FCS.

### WST-1 cell viability assay

C3A cells were seeded in 96-well plates ($10^5$ cells per well in 100 μl of the cell culture medium) and incubated for 24 h at 37°C and 5% $CO_2$. The following day the cells were exposed to the materials or controls for 24 h at 37°C, 5% $CO_2$. Subsequent to NM treatment, cell supernatants were collected and frozen at −80°C and later used for enzyme linked immunosorbent assays (ELISA) and the urea assay. Plates were washed twice with phosphate buffered saline (PBS), followed by the addition of 10 μl of the WST-1 cell proliferation reagent (Roche, Madison, USA) and 90 μl of fresh medium. Plates were then incubated for 1 h at 37°C, 5% $CO_2$. The supernatant was transferred to a fresh plate and the absorbance measured by dual wavelength spectrophotometry at 450 and 630 nm using a micro-plate reader (the supernatants were transferred into fresh plates in order to decrease the potential interference of the NMs during the measurement of the absorbance). All experiments were repeated a minimum of three times.

### AlamarBlue cell viability assay

C3A cells were plated and exposed to the selected NMs as previously described (see above). The supernatants were removed and stored at −80°C and the plates were washed twice with PBS. AlamarBlue cell proliferation reagent (Invitrogen, UK) (10 μl) and 90 μl of fresh medium was added to each well. The plates were incubated for 2 h at 37°C, 5% $CO_2$. The supernatant from each well was then transferred to a fresh plate and the absorbance measured using a spectrophotometer at a wavelength of 570 nm.

### Atomic absorption spectroscopy

Stock solution of standards was prepared for both Ag and Zn in water ranging from 4 down to 0.1 ppm. The Ag and ZnO NPs (NM 300, NM 110 and NM 111) were dispersed in the ENPRA dispersant and sonicated as previously described. To ascertain the dissolution of ZnO and Ag, the materials were diluted in both ultrapure and filtered water and C3A complete medium. The nanoparticle dispersions and blank samples were incubated in triplicate for 24 h at 37°C, 5% $CO_2$ (identical exposure conditions as used for the treatment of cells). The particles were centrifuged at 13,000 *g* for 1 h before the supernatant was passed through a 5000 kDa (25 nm) ultrafilteration column (Surrey, UK, Bohemia, NY, USA). Supernatants were stored at 4°C until accessed by atomic absorption spectroscopy (AAS).

The analysis was carried out using a Perkin Elmer AAnalyst 200 Atomic Absorption Spectrometer (Ag and Zn Hollow Cathode Lamp).

### Production of IL-8, TNF-α, IL-6, CRP and albumin

After exposure, the C3A supernatants were collected and stored at −80°C. The supernatants were centrifuged at 1000 *g* and cytokine and albumin levels determined by ELISA according to the manufacturer's instructions. Human IL-8, TNF-α and IL-6 ELISA kits were purchased from Invitrogen (Camarillo, CA, USA), human CRP ELISA from Immune Systems (Paignton, UK) and human albumin ELISA from Bethyl Laboratories (Montgomery, TX, USA).

### Impact of NMs exposure on urea production by C3A cells

In order to investigate the effects of NM exposure on urea production, a QuantiChrom Urea assay kit (BioAssay Systems, Hayward, CA, USA) was utilised. After exposure to the materials, the C3A cell supernatants were collected (see above). All samples were diluted (1:50) in distilled water and 50 μl of each sample was added to appropriate wells. Working reagent (200 μl) made from two components (reagent A: *o*-phthalaldehyde <0.40%, Brij 35 <0.04%, sulphuric acid 10% and reagent B: Primaquine diphosphate <0.08%, boric acid <0.8%, sulphuric acid 22% and Brij 35 <0.04%) was also added to all wells (1:1). The plates were incubated for 30 min at room temperature and the absorbance read at a wavelength of 430 nm on a plate reader.

### Statistical analysis

All data were expressed as mean ± standard error of the mean. For statistical analysis, the experimental results were compared with their corresponding control values using an ANOVA with Tukey's multiple comparison. All statistical analysis was carried out utilising Minitab 15. A $p$ value of <0.05 was considered to be significant. All experiments were repeated a minimum of three times.

## Results

### Characteristics of NMs and exposure media

Investigated NMs were characterised by a combination of analytical techniques in order to infer primary physical and chemical properties useful to understand their toxicological

Table II. Main physical and chemical properties of tested ENMs.

| ENP code | ENP type | Phase | XRD size (nm) | TEM size | Primary characteristics by TEM analysis | Surface area (BET) ($m^2$/g) | Known coating | Size in MEM (DLS)Ψ |
|---|---|---|---|---|---|---|---|---|
| NM 101 | $TiO_2$ | Anatase€ | 9 | 4–8/50–100 | Two structures found; type 1 show agglomerates in the 50–1500 nm range | 322 | None | 185, 742 |
| NM 110 | ZnO | Zincite | 70 to >100 | 20–250/50–350 | Mainly 2 euhedral morphologies: 1) aspect ratio close to 1 (20–250 nm range and few particles of approx. 400 nm)<br>2) Ratio 2:7.5 (50–350 nm). Minor amounts of particles with irregular morphologies observed | 14 | None | 306 |
| NM 111 | ZnO | Zincite | 58–93 | 20–200/10–450 | As NM 110, but with different size distributions. 1) Particles with aspect ratio close to 1 (~90% in the 20–200 nm range); 2) particles with aspect ratio 2:8.5 (~90% in the 10–450 nm ratio) | 18 | Triethoxycaprylylsilane 130 | 313 |
| NM 300 | Ag | Ag-metal | 7$<br>14£<br><18/15/>100# | 8–47 (av.: 17.5) | Mainly euhedral NP; minor fractions have either elongated (aspect ratio up to ~ 5) or sub-spherical morphology | NA | Polyoxylaurat Tween 20 | 12, 28, 114 |
| NM 400 | MWCNT | - | - | D: 5–35<br>L: 700–3000 | Irregular entangled kinked and mostly bent MWCNT (10–20 walls). Some CNTs were capped and in some cases multiple caps were found due to overgrowth. Fe/Co catalysts (6–9 nm, average 7.5 nm) were found inside the tubes | 298 | None | * |
| NM 402 | MWCNT | - | - | D: 6–20<br>L: 700–4000 | Entangled irregular, mostly bent MWCNT (6–14 walls). Some tubes were capped by unknown material. Some nano-onions (5–10 nm) and amorphous carbon structures mixed with Fe (5–20 nm). Residual catalyst was observed. Individual catalyst particles up to 150 nm were also detected | 225 | None | * |
| NRCWE 001 | $TiO_2$ | Rutile§ | 10 | 80–400 | Irregular euhedral particles detected by TEM | 99 | None | 203 |
| NRCWE 002 | $TiO_2$ | Rutile | 10 | 80–400 | Irregular euhedral particles detected by TEM | 84 | Positively charged | 287 |
| NRCWE 003 | $TiO_2$ | Rutile | 10 | 80–400 | Irregular euhedral particles detected by TEM | 84 | Negatively charged | 240, 1487 |
| NRCWE 004 | $TiO_2$ | Rutile | App. 100 | 1–4/10–100/100–200/1000–2000 | Five different particle types were identified: 1) irregular spheres, 1–4 nm (av. diameter); 2) irregular euhedral particles, 10–100 nm (longest dimension); 3) fractal-like structures in long chains, 100–200 nm (longest dimension); 4) big irregular polyhedral particles, 1–2 μm (longest dimension); 5) large irregular particles with jagged boundaries, 1–2 μm (longest dimension) | | | 339 |

€1% rutile found in one of the two samples analysed; $Wet XRD in capillary tube; £Dried samples; #Sample with deposits; §ca. 6% anatase was observed in one of the two samples analysed; *Not detectable by DLS due to the very large aspect ratio; ΨIntensity-based size average in biological media after 15 min; BET, Brunauer, Emmet and Teller; DLS, dynamic light scattering; ENP, engineered nanoparticles; MEM, Minimum Essential Medium Eagle; MWCNT, multi-walled carbon nanotube; NM, nanomaterial; NRCWE, National Research Centre for the Working Environment; TEM, transmission electron microscopy; XRD, X-ray diffractogram.

behaviour. A list of the measured physical and chemical properties of selected NMs is presented in Table II.

### Impact of the selected panel of NMs on C3A cell viability

From the WST-1 data it was evident that there was a dose-dependent decrease in cell viability at 24 h across the entire NMs panel (Figure 1). However, an LC50 could only be determined for exposures to Ag (NM 300) 2 μg/cm$^2$, uncoated ZnO (NM 110) 7.5 μg/cm$^2$ and coated ZnO (NM 111) 15 μg/cm$^2$ after a 24 h exposure (Figure 1B–D). The AlamarBlue data obtained also showed similar results across the 10 NMs. However, this assay gave a slightly higher LC50 value (Table IV). The WST-1 assay was relatively more sensitive over the steepest part of the curve when compared with the AlamarBlue. Silver particles (NM 300) induced the greatest level of toxicity within the C3A cells, followed by the uncoated ZnO (NM 110) and coated ZnO (NM 111) particles. All of the $TiO_2$ and MWCNT NMs were considered to be low toxicity materials as the LC50 was not reached after a 24 h exposure to the C3A cells at the range investigated.

We also investigated the toxicity of the ENPRA dispersants namely NM 300 dispersant termed (NM 300 DIS) and 0.5% ethanol in complete C3A medium. We found no toxicity of

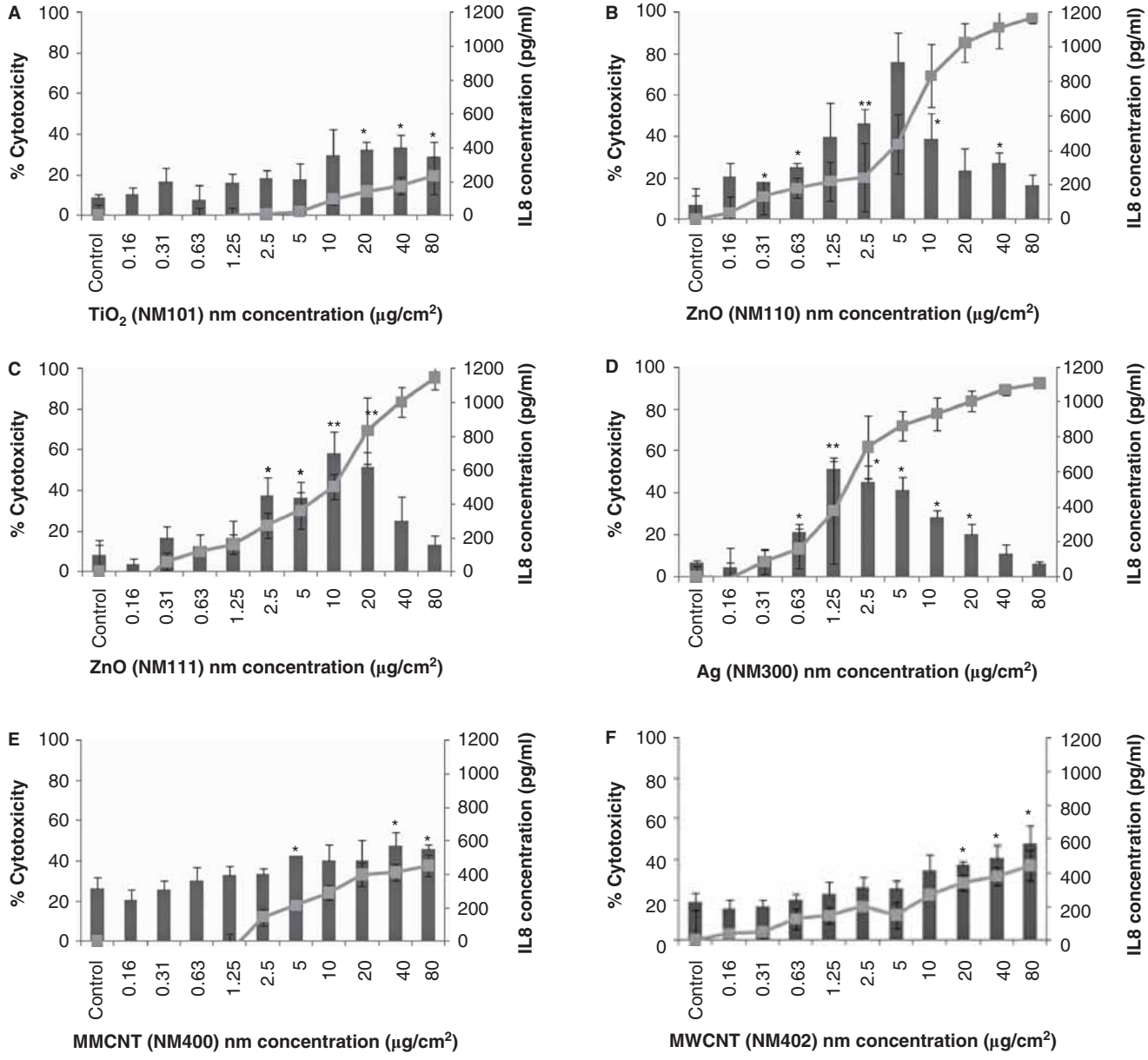


Figure 1. Cytotoxicity (grey line) and IL-8 production (black bars) by C3A cells in the presence of a panel of engineered nanomaterials. The cells were exposed to cell medium (control)/medium and dispersant for NM 300 and NMs for 24 h with cytotoxicity measured via WST-1 assay. IL-8 production within cell supernatants was measured by ELISA. Values represent mean ± SEM ($n = 3$), significance indicated by $^*p < 0.05$ and $^{**}p < 0.005$, when material treatments are compared with the control. A) NM 101; B) NM 110; C) NM 111; D) NM 300; E) NM 400; F) NM 402; G) NRCWE 001; H) NRCWE 002; I) NRCWE 003; J) NRCWE 004.

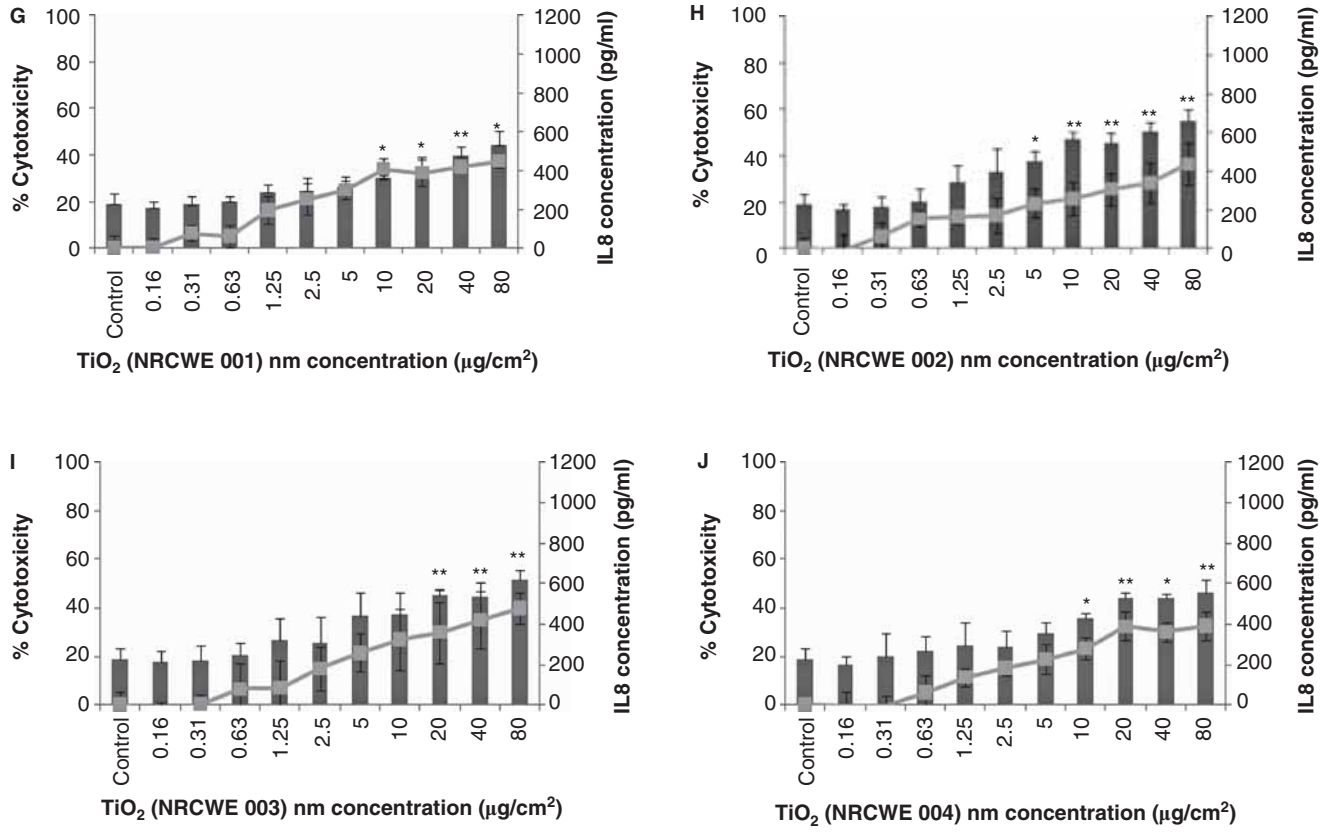


Figure 1. (*Continued*).

either dispersant to the C3A cells (data not shown), so we concluded that all observed toxicity was due to exposure to the NMs investigated.

Identifying the soluble fraction of Ag and ZnO NPs added to the cells is extremely important for the discrimination between effects induced by the NPs and dissolved elements therein. Therefore, 24 h dissolution of NM 110, NM 111 and NM 300 was investigated in pure water and the C3A complete medium at 1, 16 and 128 μg/ml (Figure 2 and Table III). We found that silver (NM 300) had a very low, but dose-dependent solubility in water ($7 \times 10^{-6}$ and $6.3 \times 10^{-4}$ mg/ml at 1 and 128 μg/ml, respectively). This solubility was slightly lower in the C3A medium ($1 \times 10^{-6}$ and $3.9 \times 10^{-4}$ mg/ml at 1 and 128 μg/ml, respectively). It is important to note that the C3A medium contained $3 \times 10^{-4}$ mg of water-soluble Zn/ml. The solubility of the NM 110 samples was between $6 \times 10^{-4}$ and $3.73 \times 10^{-4}$ mg/ml in water (1 and 128 μg/ml). In C3A medium, this concentration varied from $7 \times 10^{-4}$ to $5.92 \times 10^{-4}$ mg/ml from the lowest to the highest concentration. The solubility of NM 111 in water was lower than NM 110 ($2 \times 10^{-4}$ to $1.72 \times 10^{-4}$ mg Zn/ml from the lowest to highest concentration). These results suggest that about 50–60% of the added ZnO NMs were dissolved in the cell medium after 24 h. The amount of dissolved Ag was low and less than 1% by weight.

### Impact of the engineered NMs on C3A hepatocyte IL-8 production

Changes in cytokine production as a consequence of NM exposure were assessed within the supernatant of exposed hepatocytes and quantified via ELISA. For the low toxicity $TiO_2$ and MWCNT samples (NM 101, NM 400, NM 402, NRCWE 001, NRCWE 002, NRCWE 003 and NRCWE 004), the IL-8 production increased in a dose-dependent manner, reaching statistical significance compared with the control at high exposure concentrations (Figure 1A, E–J). However, in the presence of the highly toxic particles of Ag and ZnO (NM 110, NM 111 and NM 300), there was a significant increase in the level of IL-8 protein production that peaked around the LC50 values, followed by a decrease in the amount of the cytokine produced as the toxicity increased (Figure 1B–D).

### Impact of the NMs on C3A hepatocyte IL-6, TNF-α and CRP production

Secretion of IL-6, TNF-α and CRP into the supernatant of exposed C3A hepatocytes was quantified using ELISA analysis. There was no significant increase or decrease in the production of IL-6, TNF-α or CRP after the exposure of the C3A cells to any of the selected NMs (data not shown).

### Impact of engineered NMs on urea and albumin production by C3A hepatocytes

In order to establish whether any of the NMs affected urea and albumin production, four exposure concentrations were chosen for each material. These concentrations included the LC50 and three subsequently lower concentrations for the highly toxic particles (NM 110, NM 111 and NM 300) and two high and two low concentrations for the low toxicity NMs (80, 20, 2.5 and 0.31 μg/cm$^2$). It was observed that none of the investigated NMs were able to modify urea production

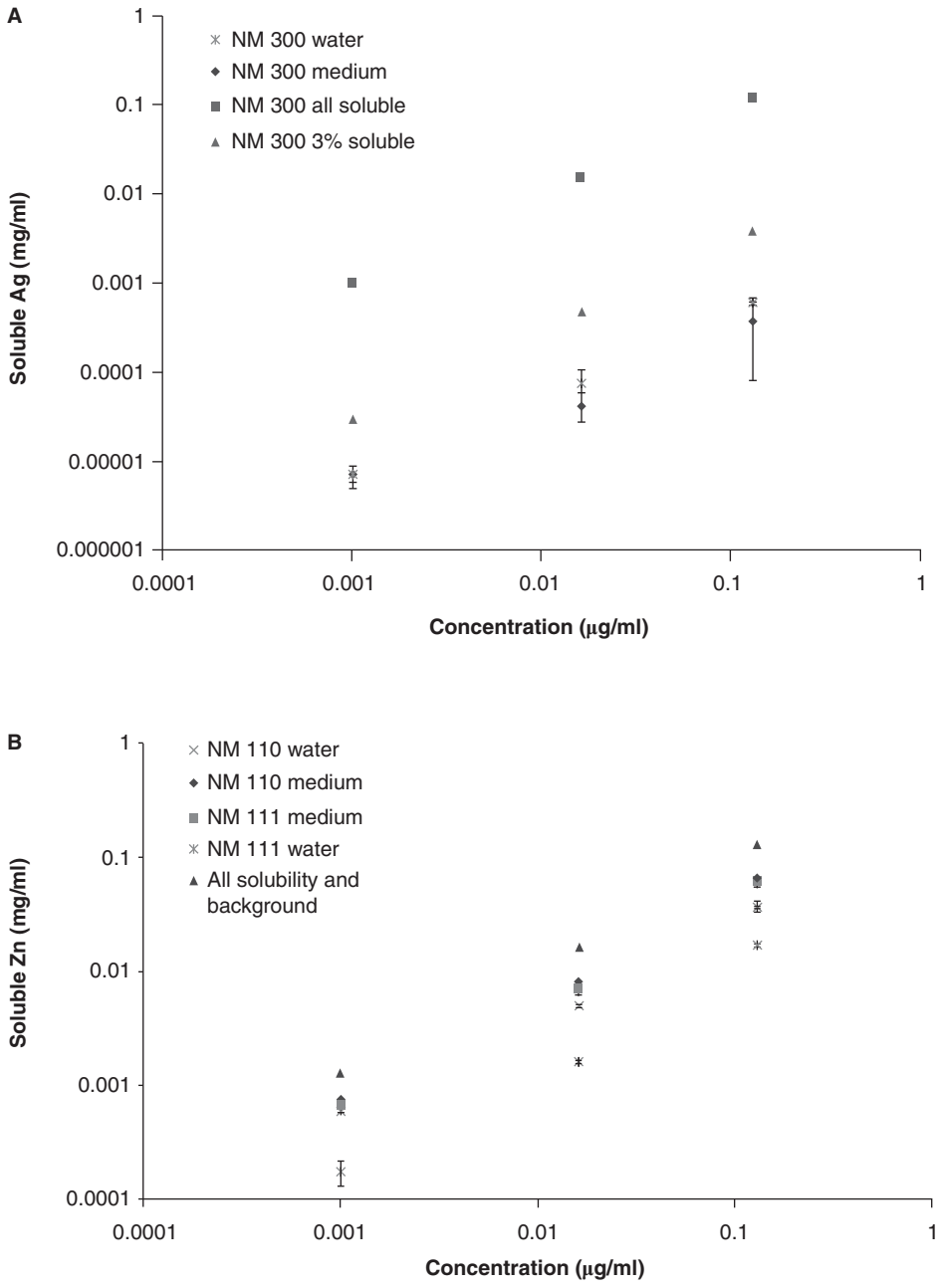


Figure 2. Ag (NM 300) and ZnO (NM 110, NM 111) nanomaterials solubility in water and C3A complete medium following 24 h of incubation at 37°C, 5% $CO_2$; 100% solubility of all three NPs is marked by triangle on each graph as reference for actual dissolution of the nanomaterials.

following a 24 h exposure period (Figure 3). There was a significant decrease in levels of albumin secreted at LC50 concentrations for both ZnO NPs – NM 110 and NM 111 (compared with the control) (Figure 3B and C). However, none of the other eight NMs were capable of affecting albumin production by hepatocytes.

## Discussion

This study was conducted as part of a large consortium (FP7 project – ENPRA) to investigate the potential hazard of a wide range of NMs on a variety of targets for risk assessment. For this reason, the wide dose response ranges

Table III. Percentage values of the Ag (NM 300) and the ZnO (NM 110, NM 111) dissolved in water and C3A complete medium following 24 h of incubation at 37°C, 5% $CO_2$.

| | NM 110 | | NM 111 | | NM 300 | |
|---|---|---|---|---|---|---|
| Treatment (μg/ml) | $H_2O$ (%) | Medium (%) | $H_2O$ (%) | Medium (%) | $H_2O$ (%) | Medium (%) |
| 1 | 59.90 | 46.70 | 17.60 | 38.90 | <0.01 | <0.01 |
| 16 | 31.68 | 33.12 | 10.06 | 25.13 | 0.78 | 0.19 |
| 128 | 29.14 | 23.36 | 13.43 | 26.48 | 0.59 | 0.47 |

Table IV. WST-1 and AlamarBlue cytotoxicity following 24 h exposure of C3A hepatocytes to NM 101 (TiO2 – 7 nm), NM 110 (ZnO – uncoated 100 nm), NM 111 (ZnO – coated 130 nm), NM 300 (Ag – <20 nm) and NM 400 (MWCNT), NM 402 (MWCNT), NRCWE 001 (TiO2 – rutile 10 nm), NRCWE 002 (TiO2 – rutile 10 nm with positive charge), NRCWE 003 (TiO2 – rutile 10 nm with negative charge) and NRCWE 004 (TiO2 – rutile 94 nm) NMs.

| | $LC_{50}$ (WST-1), μg/cm$^2$ | $LC_{50}$ (AlamarBlue), μg/cm$^2$ |
|---|---|---|
| NM 101 | $LC_{50}$ not reached up to 80 μg/cm$^2$ | $LC_{50}$ not reached up to 80 μg/cm$^2$ |
| NM 110 | $LC_{50}$ between 5 and 10 μg/cm$^2$ | $LC_{50}$ around 10 μg/cm$^2$ |
| NM 111 | $LC_{50}$ is between 10 and 20 μg/cm$^2$ | $LC_{50}$ around 20 μg/cm$^2$ |
| NM 300 | $LC_{50}$ is between 1.25 and 2.5 μg/cm$^2$ | $LC_{50}$ is between 2.5 and 5 μg/cm$^2$ |
| NM 400 | $LC_{50}$ not reached up to 80 μg/cm$^2$ | $LC_{50}$ not reached up to 80 μg/cm$^2$ |
| NM 402 | $LC_{50}$ not reached up to 80 μg/cm$^2$ | $LC_{50}$ not reached up to 80 μg/cm$^2$ |
| NRCWE 001 | $LC_{50}$ not reached up to 80 μg/cm$^2$ | $LC_{50}$ not reached up to 80 μg/cm$^2$ |
| NRCWE 002 | $LC_{50}$ not reached up to 80 μg/cm$^2$ | $LC_{50}$ not reached up to 80 μg/cm$^2$ |
| NRCWE 003 | $LC_{50}$ not reached up to 80 μg/cm$^2$ | $LC_{50}$ not reached up to 80 μg/cm$^2$ |
| NRCWE 004 | $LC_{50}$ not reached up to 80 μg/cm$^2$ | $LC_{50}$ not reached up to 80 μg/cm$^2$ |

MWCNT, multi-walled carbon nanotube; NM, nanomaterial; NRCWE, National Research Centre for the Working Environment.



were used in order to allow calculation of values such as LC50 for comparisons between different materials and cell target types both *in vitro* and *in vivo*.

This particular study focused on the impacts of the investigated NMs panel on hepatocytes with respect to cytotoxicity, pro-inflammatory cytokine production and markers of function. The data show that the NMs vary in terms of their toxicity and impact on cell function after acute (24 h) exposure *in vitro*.

This acute *in vitro* cytotoxicity study indicates that the NM panel can be segregated into a low ($TiO_2$ and MWCNT) and a high toxicity group (Ag and coated and uncoated ZnO) (Table IV). The silver NPs were the most toxic with an LC50 as low as 2 μg/cm$^2$. Our results are similar to previous studies in which hepatocytes exposed to uncoated 5–10 nm Ag particles for a period of 24 h were toxic at concentrations as low as 0.5 μg/ml (Kawata et al. 2009; Park et al. 2010). It has been shown that at nanoscale, silver exhibits remarkably unusual physical, chemical and biological properties (Chen et al. 2008).

The coated and uncoated ZnO NPs also exhibited significant toxicity to cells (NM 110 – LC50 7.5 μg/cm$^2$ and NM 111 – LC50 15 μg/cm$^2$). In a recent set of trials, it was shown that ZnO NPs have significant toxic effects on aortic endothelial cells, with 50% of cells dying after a 4 h incubation period with 50 nm particles (Gojovo et al. 2007). In another study on mouse neural stem cells, a 24 h incubation with 30, 60 and 200 nm ZnO particles resulted in manifestation of a clear dose-dependent toxicity to the cells (LC50 8–20 μg/cm$^2$). The authors proposed that the ZnO induced apoptosis of the treated cells (Deng et al. 2009).

Both Ag and ZnO have been reported elsewhere to exhibit solubility resulting in the release of ions that contribute to the toxicity of these NMs (Fabrega et al. 2011; Kim et al. 2011; Song et al. 2010; Wong et al. 2010; Zheng et al. 2011). Our assessment of dissolution in complete C3A medium showed that the less than 1% of Ag (NM 300) dissolves in this medium after 24 h of incubation so it is very unlikely that the toxicity witnessed is due to the release of ions. Similarly in a recent study in which A549 (alveolar cell line) were exposed to both Ag NPs and ions in a dose-dependent manner. The authors noted very low toxicity following exposure to the $Ag^+$ at the lower concentrations (Foldbjerg et al. 2011). Our Ag solubility findings are similar to previous studies in which it was noted that very little silver is dissolved in the tested media (Chappell et al. 2011; Gaiser et al. 2011). However, we observed that the two ZnO NPs (NM 110 and NM 111) were partially soluble in the medium utilised so there is a real possibility that the high toxicity of these particles is in part due to the release of ions. Around 50–60% of the added ZnO NMs were found as soluble Zn in the cell medium utilised. Some soluble Zn (2.9 μg/ml) was already present in the original cell medium, but addition of the NM 110 and NM 111 increased the concentrations in a dose-dependent manner up to 128 μg/ml in the cell medium. Further understanding of the dissolution kinetics of these partially soluble compounds in both the test item preparation step and in the cell mediums are crucial for further understanding of the toxicology of these NMs.

It has been suggested that in sufficient doses $TiO_2$ can cause pulmonary inflammation, fibrosis and damage (Jin et al. 2008). Based on recent *in vivo* studies, inflammation may persist for several months, but does not reach the level of inflammation induced by quartz (Roursgaard et al. 2011). It has also been shown that after translocation from the primary site of exposure, the NPs can induce oxidative stress-mediated toxicity in many cell types by producing large amounts of free radicals (Jin et al. 2008; Kang et al. 2008; Wang et al. 2007). We found all five $TiO_2$ were of relatively low toxicity to the C3A cells (LC50 was not reached in the presence of any of the NPs up to 80 μg/cm$^2$). Similarly, in a study using Caco-2 cells it was found that there was no cytotoxicity following 24 h exposure to $TiO_2$ NPs (Jin et al. 2008). Xia et al. (2006) discovered that $TiO_2$ nanoparticles did cross the epithelial lining of the intestinal model by transcytosis, albeit at low levels. $TiO_2$ was able to penetrate into and through the cells without disrupting junctional complexes. It is also interesting to note that a recent study suggests that $TiO_2$ NM exposure did not result in any toxicological effects to mammalian cells under dark conditions (Koeneman et al. 2010). Our exposures here were also conducted in the dark. In addition, the data presented here indicate that relatively high $TiO_2$ exposure concentrations can induce production of the pro-inflammatory cytokine IL-8, which agrees with other *in vitro* studies (Monteiller et al. 2007).

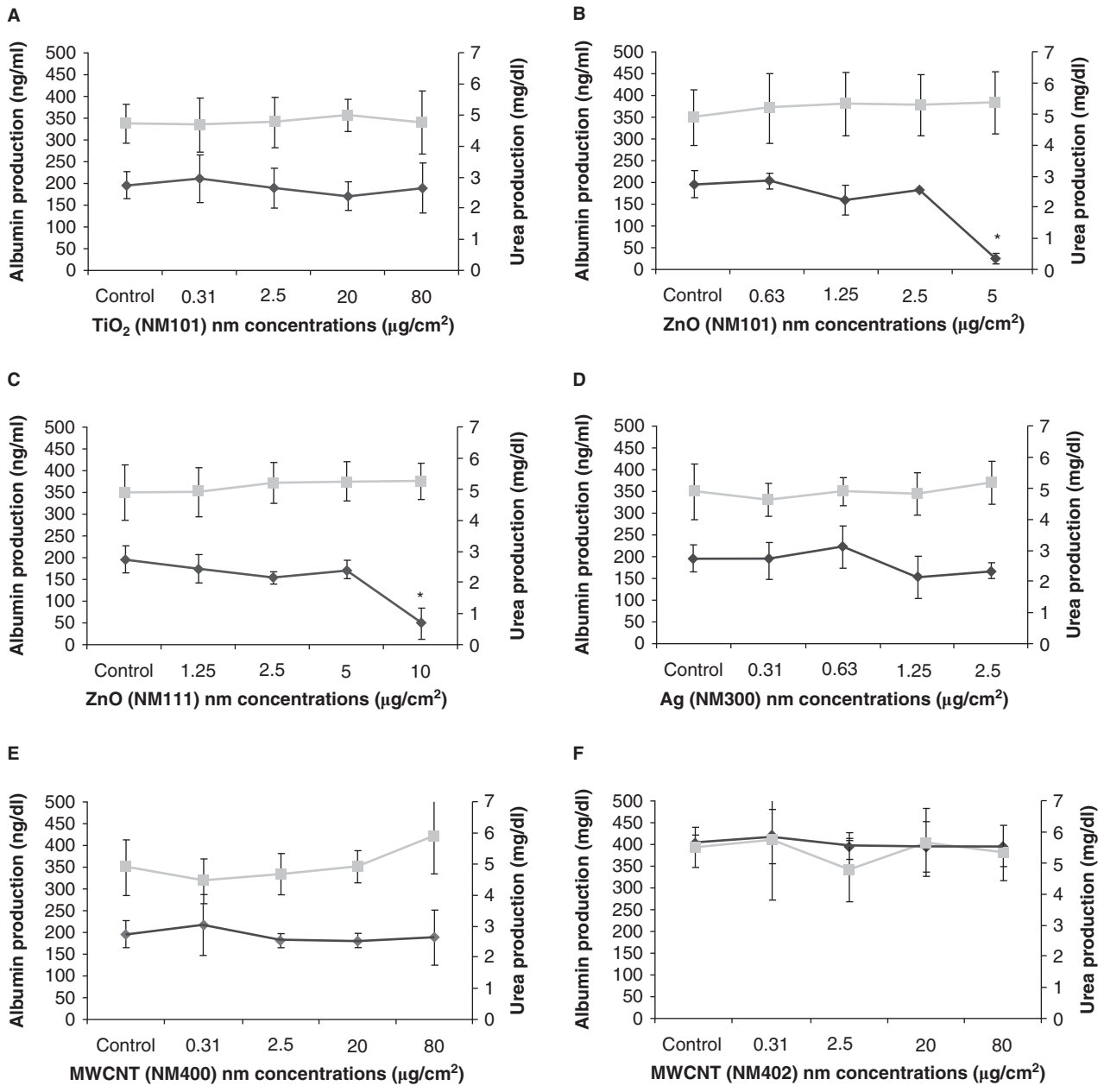


Figure 3. Albumin production (black line) and urea secretion (grey line) from C3A cells in the presence of a panel of engineered nanomaterials. Cells were exposed to medium (control) or NMs for 24 h. Values represent mean ± SEM ($n = 3$), significance indicated by $^*p < 0.05$, compared with the control. A) NM 101; B) NM 110; C) NM 111; D) NM 300; E) NM 400; F) NM 402; G) NRCWE 001; H) NRCWE 002; I) NRCWE 003; J) NRCWE 004.

Finally, we found that the MWCNTs tested were relatively non-toxic to the C3A cells at the times and concentrations tested. The toxicity of MWCNTs is widely documented, with adverse effects observed as pulmonary inflammogenicity (Ellinger-Ziegelbauer et al. 2009), hepatotoxicity (Ji et al. 2009), dermal and ocular irritation (Kishore et al. 2009) as well as monocyte (De Nicola et al. 2009) and macrophage (Hirano et al. 2008) mediated pathogenesis to name but a few. Like other NMs, CNTs may be capable of entering the bloodstream and can be translocated to secondary organs. Most of the manufactured MWCNTs are of an inhalable size and although most dust by mechanical agitation is coarse they could be potentially dangerous to anyone exposed (Hoet et al. 2004). It has been suggested that the cytotoxicity of SWCNTs is higher than that of MWCNTs (Shvedova et al. 2005), yet *in vitro* exposure of RAW264.7 macrophage cell line to SWCNTs was associated with the active production of transforming growth factor β and reduced levels of the pro-inflammatory cytokines TNF-α and IL-1-β (Shvedova et al. 2005). The authors also did not witness any ROS activity (Shvedova et al. 2005). The data presented here also support the activity of MWCNT to induce the production of the pro-inflammatory cytokine IL-8, but only at relatively high exposure concentrations.

Although some NMs absorb proteins and form a protein corona (Montes-Burgos et al. 2010) which could influence uptake and fate of the particle, we believe it is physiologically more relevant for the hepatocytes to be exposed to the NMs

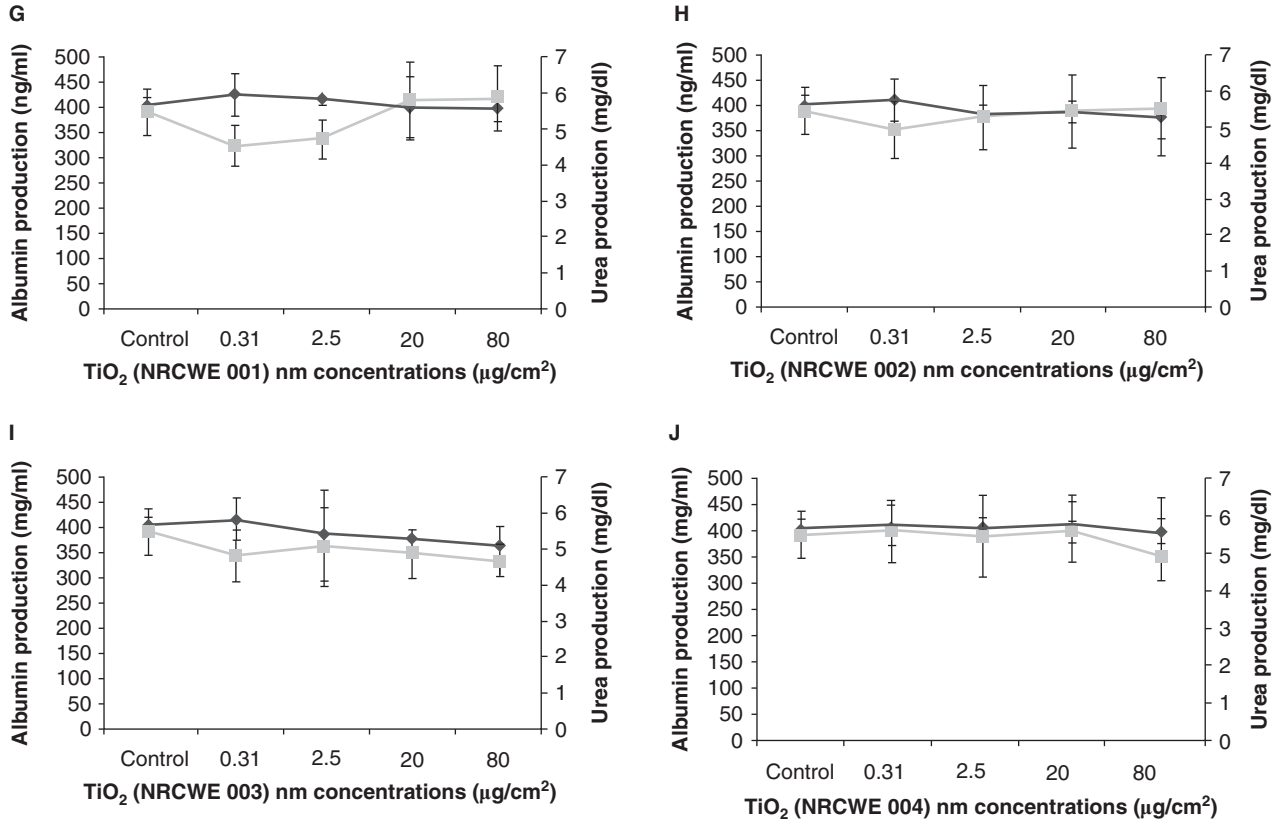


Figure 3. (*Continued*).

in a medium containing serum as for any NMs to reach the liver, it will be exposed to numerous proteins along the way. In addition, the C3A cells require 10% serum to survive *in vitro*.

The ability of NMs to compromise the viability of the C3A was investigated using both the WST-1 and AlamarBlue assays. The WST-1 assay is based on the enzymatic cleavage of tetrazolium salt to a water-soluble formazan dye by the mitochondria (tetrazolium reductase) in viable cells. An expansion in the number of viable cells results in an increase of overall activity of mitochondrial dehydrogenases, hence more WST-1 is converted to the formazan which can be detected and quantified. This absorbance value is representative of cell viability (Al-Nasiry et al. 2007). AlamarBlue is a non-toxic, cell-permeating compound that is blue in colour and virtually non-fluorescent. On entering cells, resazurin is reduced to resorufin, which produces very bright red fluorescence. Viable cells continuously convert resazurin to resorufin, thereby generating a quantitative measure of viability and cytotoxicity (Al-Nasiry et al. 2007). Although data gathered revealed both assays were very similar across the 10 NMs, WST-1 was more sensitive over the steepest part of the curve when compared with the AlamarBlue assay.

Hepatocytes are responsible for the manufacture of important serum proteins. They play a substantial role in the metabolism of lipids (Kmiec et al. 2001) and synthesise many hormones and cytokines including IL-8 (Dong et al. 1998), IL-6 (Saad et al. 1995), TNF-α (Saad et al. 1995) and CRP (Vermeire et al. 2005). IL-8 is a chemokine mediating the activation and migration of a wide variety of inflammatory cells including macrophages and mast cells into tissue, hence playing a pivotal role in initiation of an inflammatory response (Puthothu et al. 2006). As described above, we discovered a significant increase in the levels of IL-8 produced by the C3A cells in the presence of NMs, with these levels peaking around the LC50 mark for the highly toxic particles (Ag and the two ZnO NPs). The decrease in cytokine production at concentrations above the LC50 in the presence of the toxic concentrations of NPs is likely due to the fact the cells were dying preventing cytokine production. In the presence of low toxicity NMs ($TiO_2$ and MWCNT), C3A cells produced increased levels of IL-8 peaking only at the highest concentrations suggesting that they cause a lower pro-inflammatory response than Ag and ZnO. These experiments seem to suggest that the *in vitro* hepatocyte NM-induced inflammation seems to include IL-8 production from the cells. It is interesting to note that exposure of the liver cell line HepG2 to microorganisms (*Brucella*) *in vitro* also resulted in an increase of IL-8 secretion from the cells (Delpino et al. 2010). These findings suggest that IL-8 seems to mediate hepatocyte inflammation in response to a number of stress factors, including NMs.

We found no change in the levels of IL-6, TNF-α or CRP following exposure of the C3A cells to any of the investigated NMs suggesting that the inflammatory response is limited. There is a real possibility that for a more realistic representation of cytokine secretion in the liver incorporation of other cells (i.e., Kupffer cells) into the *in vitro* system might be essential (Sadauskas et al. 2007). This will form the basis of a future study.

Both urea and albumin were quantified as measures of liver function. Following exposure of C3A cells to the panel of NMs, it was discovered that there was no significant decrease or increase in the levels of urea production. We also found that there was no change in the levels of albumin following NM exposure, with the exception of both ZnO NPs. These results suggest that with the exception of ZnO, despite varying degrees of cell death, none of the NMs investigated affected hepatocyte function *in vitro* in terms of albumin and urea production. It is interesting that although silver was the most toxic NM investigated in terms of viability, this did not translate into the effect on cell function at sub-lethal concentrations.

## Conclusions

In conclusion, the *in vitro* hepatocyte model demonstrated that Ag and ZnO NPs were consistently more potent with respect to cytotoxicity and cytokine production. In comparison, the MWCNT and $TiO_2$ NMs investigated revealed relatively lower toxicity. The cytotoxicity of ZnO may be related to its solubility, but this is less likely for the Ag NPs. Future hepatocyte studies will concentrate on DNA damage and ascertaining the potential mechanism driving inflammation in particular the role of reactive oxygen species in C3A cells post NM exposure. Studies conducted by project partners will employ other target cells such as macrophages, lung epithelial cells, fibroblasts, endothelial cells and renal proximal tubule epithelial cells. *In vivo* studies are also being conducted for comparison with *in vitro* models. All of these data will be combined into a database to be used in risk assessment.



## Acknowledgements

This work has been financially supported by the European seventh framework programme co-operation (Grant code – NMP4-SL-2009-228789). The authors are grateful to colleagues at Heriot-Watt University and Edinburgh Napier University. The authors would also like to thank Andrea Brunelli and Davide Cristofori (University Ca' Foscari Venice) for their technical support during characterisation of the nanomaterials.

## Declaration of interest

The authors report no conflicts of interest. The authors alone are responsible for the content and writing of the paper.

## References

Al-Nasiry S, Geusens N, Hanssens M, Luyten C, Pijnenborg R. 2007. The use of Alamarblue assay for quantitative analysis of viability, migration and invasion of choriocarcinoma cells. Hum Reprod 22: 1304–1309.

Brunauer PH, Emmet H, Teller E. 1938. Adsorption of gases in multi-molecular layers. J Am Chem Soc 60:309–315.

Buzea C, Pacheco II, Robbie K. 2007. Nanomaterials and nanoparticles: sources and toxicity. Biointerpahses 2:18–67.

Chappell MA, Miller LF, George AJ, Pettway BA, Prince CL, Porter BE, et al. 2011. Simultaneous dispersion-dissolution behaviour of concentrated silver nanoparticle suspensions in the presence of model organic solutes. Chemosphere 84:1108–1116.

Chen C, Zhang P, Hou X, Chai Z. 1999. Sub-cellular distribution of selenium and Se-containing proteins in human liver. Biochem Biophys Acta 1427:205–215.

Chen X, Schluesener HJ. 2008. Nanosilver: a nanoproduct in medical application. Toxicol Lett 176:1–12.

De Nicola M, Nuccitelli S, Gattia DM, Traversa E, Magrini A, Bergamaschi A, et al. 2009. Effects of carbon nanotubes on human monocytes. Natural Compounds and their Role in Apoptotic Cell Signalling Pathways. 1171:600–605.

Delpino MV, Barrionuevo P, Scian R, Fossati CA, Balsi PC. 2010. Brucella-infected heaptocytes mediate potentially tissue-damaging immune responses. J Hepatol 53:145–154.

Deng X, Luan Q, Chen W, Wang Y, Wy M, Zhang H, et al. 2009. Nanosized zinc oxide particles induce neural stem cell apoptosis. Nanotechnology 20:1–7.

Dong BW, Liang P, Yu XL, Zeng XQ, Wang PJ, Su L, et al. 1998. Sonographically guided microwave coagulation treatment of liver cancer: an experimental and clinical study. Am J Roentgenol 171:449–454.

Ellinger-Ziegelbauer H, Pauluhn J. 2009. Pulmonary toxicity of multi-walled carbon nanotubes (Baytubes(R)) relative to alpha-quartz following a single 6 hour inhalation exposure of rats and a 3 months post-exposure period. Toxicology 226:16–29.

Fabrega J, Luoma SN, Tyler CR, Galloway TS, Lead R. 2011. Silver nanoparticles: behaviour and effects in the aquatic environment. Environ Int 37:517–531.

Ferrari M. 2005. Cancer nanotechnology: opportunities and challenges. Nat Rev Cancer 9:343–346.

Foldbjerg R, Dang DA, Autrup H. 2011. Cytotoxicity and genotoxicity of silver nanoparticles in human lung cancer line, A549. Arch Toxicol 85:743–750.

Gaiser BK, Biswas A, Rosenkranz P, Jepson MA, Lead JR, Stone V, et al. 2011. Effects of silver and cerum oxide micro and nano sized particles on Daphnia magna. J Environ Monit 13:1227–1235.

Gaiser BK, Fernandes TF, Jepson M, Lead JR, Tyler CR, Stone V. 2009. Assessing exposure, uptake and toxicity of silver and cerium dioxide nanoparticles from contaminated environments. Environ Health 8 (Suppl 1).

Geiser M, Kreyling WG. 2010. Deposition and biokenetics of inhaled nanoparticles. Part Fibre Toxicol 7:2–19.

Gekle M. 2005. Renal tubule albumin transport. Annu Rev Physiol 67:573–594.

Gojovo A, Guo B, Kota RS, Rutledge JC, Kennedy IM, Barakat AI. 2007. Induction of inflammation in vascular endothelial cells by metal oxide nanoparticles: effect of particle composition. Environ Health Perspect 115:403–409.

Hirano S, Kanno S, Furuyama A. 2008. Multi-walled carbon nanotubes injure the plasma membrane of macrophages. Toxicol Appl Pharmacol 232:244–251.

Hoet PHM, Hohlfeld IB, Salata O. 2004. Nanoparticles – known and unknown health risks. J Nanobiotechnology 2:12–27.

Huang Z, Zheng X, Yan D, Yin G, Liao X, Kang Y, et al. 2008. Toxicological effect of ZnO nanoparticles based on bacteria. Langmuir 24:4140–4144.

Jacobsen NR, Pojano G, Wallin H, Jensen KA. 2010. Nanomaterial dispersion protocol for toxicological studies in ENPRA. Internal ENPRA Project Report. Natl Res Centre Working Environ 6: Internal ENPRA report P1–10.

Jensen KA, Bilaničová D, Birkedal R, Pojana G, Marcomini A, Wallin H, et al.Optimization and evaluation of a generic nanoparticle dispersion protocol for in vitro and in vivo toxicity testing using serum-water. Manuscript in preparation.

Ji Z, Zhang D, Li L, Shen X, Deng X, Dong L, et al. 2009. The hepatotoxicity of multi-walled carbon nanotubes in mice. Nanotechnology 20:445101.

Jin CY, Zhu BS, Wang XF, Lu QH. 2008. Cytotoxicity of Titanium dioxide nanoparticles in mouse fibroblast cells. Chem Res Toxicol 21:1871–1877.

Kang SJ, Kim BM, Lee YJ, Chung HW. 2008. Titanium dioxide nanoparticles trigger p53-mediated damage response in peripheral blood lymphocytes. Environ Mol Mutagen 49:399–405.

Kawata K, Osawa M, Okabe S. 2009. In vitro toxicity of silver nanoparticles at noncytotoxic doses to HepG2 human hepatoma cells. Environ Sci Technol 43:6046–6051.

Kim J, Kim S, Lee S. 2011. Differentiation of the toxicities of silver nanoparticles and silver ions to the Japanese medaka (Oryzias latipes) and the cladoceran Daphnia magna. Nanotoxicology 5:208–214.

Kishore AS, Surekha P, Murthy PB. 2009. Assessment of the dermal and ocular irritation potential of multi-walled carbon nanotubes by using in vitro and in vivo methods. Toxicol Lett 191:268–274.
Kmiec Z. 2001. Co-operation of liver cells in health and disease. Adv Anat Embryol Cell Biol 161, 1–151.
Koeneman BA, Zhang Y, Westerhoff P, Chen Y, Crittenden JC, Capco DG. 2010. Toxicity and cellular responses of intestinal cells exposed to titanium dioxide. Cell Biol Toxicol 26:225–238.
Loeschner K, Hadrup N, Qvortrup K, Larsen A, Gao X, Vogel U, et al. 2011. Distribution of silver in rats following 28 days of repeated oral exposure to silver nanoparticles or silver acetate. Part Fibre Toxicol 8:18–32.
Maynard AD, Aitkin RJ, Butz T, Colvin V, Donaldson K, Oberdorster G, et al. 2006. Safe handling of nanotechnology. Nature 444:267–269.
Monteiller C, Tran L, MacNee W, Faux S, Jones A, Miller B, et al. 2007. The pro-inflammatory effects of low toxicity low solubility particles, nanoparticles and fine particles, on epithelial cells in vitro: the role of surface area. Occup Environ Med 64:609–615.
Montes-Burgos I, Walcyzk D, Hole P, Smith J, Lynch I, Dawaon K. 2010. Characterisation of nanoparticle size and state prior to nanotoxicological studies. J Nanopart Res 12:47–53.
Oberdorster G, Maynard A, Donaldson K, Castranova V, Fitzpatrick J, Ausman K, et al. 2005. Principles for characterizing the potential human health effects from exposure to nanomaterials: elements of a screening strategy. Part Fibre Toxicol 42:1–35.
Oberdorster G, Oberdorster E, Oberdorster J. 2005. Nanotoxicology: an emerging discipline evolving from studies of ultrafine particles. Environ Health Perspect 113:823–839.
Park EJ, Yi J, Kim Y, Choi K, Park K. 2010. Silver nanoparticles induce cytotoxicity by a Trojan-horse type mechanism. Toxicol In Vitro 24:872–878.
Puthothu B, Krueger M, Heinze J, Forster J, Heinzmann A. 2006. Impact of IL8 and IL8-receptor alpha polymorphisms on the genetics of bronchial asthma and severe RSV infections. Clin Mol Allergy 4:2–8.
Rhodes B, Furnrohr BG, Vyse TJ. 2011. C-reactive protein in rheumatology: biology and genetics. Nat Rev Rheumatol 7:282–289.
Roselli M, Finamore A, Garaguso I, Britti MS, Mengheri E. 2003. Zinc oxide protects cultured enterocytes from the damage induced by Escherichia coli. J Nutr 133:4077–4082.
Roursgaard M, Jensen KA, Poulsen SS, Jensen NEV, Poulsen LK, Hammer M, et al. 2011. Acute and subchronic airway inflammation after intratracheal instillation of quartz and titanium dioxide agglomerates in mice. ScientificWorld Journal 11:801–825.
Saad B, Frei K, Scholl FA, Fontana A, Maier P. 1995. Hepatocyte-derived interleukin-6 and tumour-necrosis factor alpha mediate the lipopolysaccharide-induced acute-phase response and nitric oxide release by cultured rat hepatocytes. Eur J Chem 229:349–355.
Sadauskas E, Jacobson NR, Danscher G, Soltenberg M, Larsen A, Kreyling W, et al. 2009. Bio-disruption of gold nanoparticles in mouse lung following intratracheal instillation. Chem Cent J 3:16–23.
Sadauskas E, Wallin H, Stoltenberg M, Vogel U, Doering P, Larsen A, et al. 2007. Kupffer cells are central in the removal of nanoparticles from the organism. Part Fibre Toxicol 4:10–17.
Sandhiya S, Dkhar SA, Surendiran A. 2009. Emerging trends of nanomedicine - an overview. Fundam Clin Pharmacol 23:263–269.
Semmler-Behnke M, Wolfgang KG, Lipka J, Fertsch S, Wenk A, Takeneka S, et al. 2008. Bio-distribution of 1.4 and 18 nm gold particles in rats. Small 12:2108–2111.
Shvedova AA, Kisin ER, Mercer R, Murray AR, Johnson VJ, Potapovich AI, et al. 2005. Unusual inflammatory and fibrogenic pulmonary responses to single walled carbon nanotubes in mice. Am J Physiol 289:698–708.
Song WH, Zhang JY, Guo J, Zhang JH, Ding F, Li LY, et al. 2010. Role of dissolved zinc ion and reactive oxygen species in cytotoxicity of ZnO nanoparticles. Toxicol Lett 199:389–397.
Takenaka S, Karg E, Moller W, Roth C, Ziesenis A, Heinzmann U, et al. 2001. Pulmonary and systemic distribution of inhaled ultrafine silver particles in rats. Environ Health Perspect 4:547–551.
Vermeire S, Van Assche G, Rutgeerts P. 2005. The role of C-reactive protein as an inflammatory marker in gastrointestinal diseases. Nat Clin Pract Gastroenterol Hepatol 2:580–586.
Wang JJ, Sanderson BJ, Wang H. 2007. Cyto- and genotoxicity of ultrafine $TiO_2$ particles in cultured human lymphoblastoid cells. Mutat Res 628:99–106.
Wong SWY, Leung PTY, Djurisic AB, Leung KMY. 2010. Toxicities of nano zinc oxide of five marine organisms: influences of aggregate sizes and ion solubility. Anal Bioanal Chem 396:609–618.
Woodrow Wilson. http://www.nanotechproject.org/inventories/consumer/browse/products/ Accessed 10 May 2011.
Xia T, Kovochich M, Brant J, Hotze M, Sempf J, Oberley T, et al. 2006. Comparison of the abilities of ambient and manufactured nanoparticles to induce cellular toxicity according to an oxidative stress paradigm. Nano Lett 6:1794–1807.
Zheng XO, Wu R, Chen YG. 2011. Effects of ZnO nanoparticles on wastewater biological nitrogen and phosphorous removal. Environ Sci Technol 45:2826–2832.